

Large-scale brain simulations on the desktop using procedural connectivity

James C Knight^{a,1} and Thomas Nowotny^a

^aCentre for Computational Neuroscience and Robotics, School of Engineering and Informatics, University of Sussex, Brighton, United Kingdom

This manuscript was compiled on March 20, 2020

Large-scale simulations of spiking neural networks are important for improving our understanding of the dynamics and ultimately function of brains. However, even small mammals such as mice have approximately 1×10^{12} synaptic connections which are typically characterized by at least one floating point value per synapse. This amounts to several terabytes of connection data – an unrealistic memory requirement for a single desktop machine. Simulations of large spiking neural networks are therefore typically executed on large distributed supercomputers. This is costly and limits large-scale modelling to a select few research groups with the appropriate resources. In this work, we describe extensions to GeNN – our GPU-based spiking neural network simulator – that enable it to ‘procedurally’ generate connectivity and synaptic weights ‘on the go’ as spikes are triggered, instead of storing and retrieving them from memory. We find that GPUs are well-suited to this approach because of their raw computational power, which due to memory bandwidth limitations is often under-utilised when simulating spiking neural networks. We demonstrate the value of our approach with a recent model of the Macaque visual cortex consisting of 4.13×10^6 neurons and 24.2×10^9 synapses. Using our new method, this model can be simulated on a single GPU. Our results match those obtained on a supercomputer and the simulation runs faster on a single high-end GPU than a previous simulation executed on over 1000 supercomputer nodes.

spiking neural networks | GPU | high-performance computing | brain simulation

The brain of a mouse has around 70×10^6 neurons, but this number is dwarfed by the 1×10^{12} (1) synapses which connect them. In computer simulations of spiking neural networks, propagating spikes through synapses involves reading a ‘row’ of synapses connecting a spiking presynaptic neuron to its postsynaptic partners and adding the ‘weight’ of each synapse in the row to a ‘bin’ containing the postsynaptic neuron’s input for the next simulation timestep. Typically, the information describing which neurons are connected by a synapse and with what conductance, is generated before a simulation is run and stored in large matrices in random access memory (RAM). This creates high memory requirements for large-scale brain models, so that they can typically only be simulated on large distributed computer systems using software such as NEST (2) or NEURON (3). By careful design, these simulators can keep the memory requirements for each node constant, even when a simulation is distributed across thousands of nodes (4). However, high performance computer systems are bulky, expensive and consume large amounts of power, meaning that they are typically shared resources that are only accessible to a limited number of researchers and for strongly time-limited investigations.

Neuromorphic systems (5–10) take inspiration from the brain and have been developed specifically for simulating

large spiking neural networks. One particular relevant feature of the brain is that its memory elements – the synapses – are co-located with the computing elements – the neurons – throughout the entire system. In neuromorphic systems, this often translates to dedicating a large proportion of each chip to memory. However, while such on-chip memory is fast, it can only be fabricated at relatively low density meaning that many of these systems economize – either by reducing the maximum number of synapses per neuron to as few as 256 or by reducing the precision of the synaptic weights to 6 (10), 4 (5) or even 1 bit (6, 8). Such strategies allow some classes of spiking neural networks to be simulated very efficiently, but reducing the degree of connectivity in large-scale brain simulations to fit within the constraints of current neuromorphic systems inevitably changes their dynamics (11). Unlike the majority of other neuromorphic systems, the SpiNNaker (7) neuromorphic super-computer is entirely programmable and combines a large amount of on-chip memory with external memories, distributed across the system for the storage of synaptic connectivity. SpiNNaker’s external memory bandwidth, on-chip memory capacity and the computational power of each core are all tailored to large-scale brain simulation meaning that the output bins of the synapse processing algorithm can fit in on-chip memory and there is enough external memory bandwidth to fetch synaptic rows fast enough for real-time simulation of large-scale models (12). This is a promising approach for future research but, because of its prototype nature, the availability of SpiNNaker hardware is limited and a physically large system is still required for even moderately-sized simulations (9 boards for a simulation with around 10×10^3 neurons and 300×10^6 synapses (12)).

Modern GPUs have relatively small amounts of on-chip memory and, instead, dedicate the majority of their silicon area to arithmetic logic units (ALUs). GPUs use dedicated

Significance Statement

Authors must submit a 120-word maximum statement about the significance of their research paper written at a level understandable to an undergraduate educated scientist outside their field of speciality. The primary goal of the Significance Statement is to explain the relevance of the work in broad context to a broad readership. The Significance Statement appears in the paper itself and is required for all research papers.

J.K. and T.N. wrote the paper. T.N. is the original developer of GeNN. J.K. is currently the primary GeNN developer and was responsible for extending the code generation approach to the procedural simulation of synaptic connectivity. J.K. performed the experiments and the analysis of the results that are presented in this work.

The authors declare no conflict of interest.

¹To whom correspondence should be addressed. E-mail: J.C.Knightsussex.ac.uk

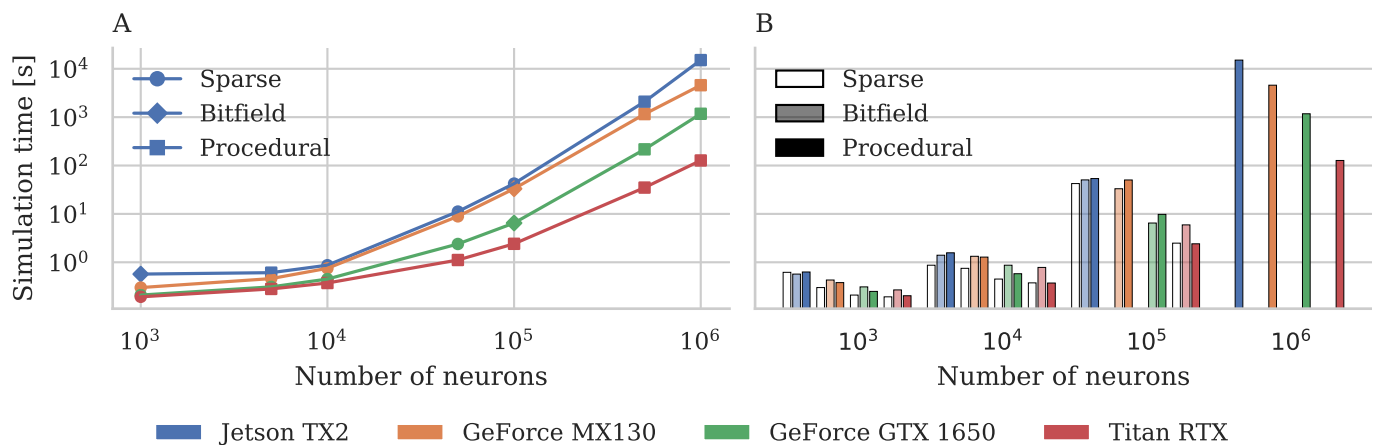


Fig. 1. Simulation time performance scaling on a range of modern GPUs (colors). **A** The best performing approach at each scale on each GPU (indicated by the symbols). For the largest models, the procedural method is always best. **B** Raw performance of each approach on each GPU. Missing bars indicate insufficient memory to simulate.

hardware to rapidly switch between tasks so that the latency of accessing external memory can be ‘hidden’ behind computation, as long as there is sufficient computation to be performed. For example, the memory latency of a typical modern GPU can be completely hidden if each CUDA core performs approximately 10 arithmetic operations per byte of data accessed from memory. Unfortunately, processing a synapse in a spiking neural network simulation is likely to require accessing approximately 8 B of memory and performing many fewer than the required 80 instructions. This makes synaptic updates highly memory bound. Nonetheless, we have shown in previous work (13) that, as GPUs have significantly higher total memory bandwidth than even the most expensive CPU, moderately sized models of around 10×10^3 neurons and 1×10^9 synapses can be simulated on a single GPU with competitive speed and energy requirements. However, individual GPUs do not have enough memory to simulate truly large-scale brain models and, although small numbers of GPUs can be connected together using the high-speed NVLink (TODO: cite) interconnect, beyond such small GPU clusters, scaling will be dictated by the same communication overheads as for other MPI-based distributed systems.

In this work we present a novel approach which converts large-scale brain simulation from a problem which is memory-bound on a GPU to one where the large amount of computational power available on a GPU can be used to reduce both memory and memory bandwidth requirements and enable truly large-scale brain simulations on a single GPU workstation.

Results

In the following subsections, we will first present two recent innovations in our GeNN simulator (14) which allow it to be used for simulating large-scale models on a single GPU. We will then demonstrate the power of these new features by simulating a recent model of the Macaque visual cortex (15) consisting of 4.13×10^6 neurons and 24.2×10^9 synapses on a single GPU. We find that we not only obtain the same results as in the previous simulation on a high-performance supercomputer, but our simulation also runs faster.

Procedural connectivity. Our GeNN simulator (14) uses code generation to convert neuron and synapse models – described

using ‘snippets’ of C-like code – into CUDA code for GPU simulation. We previously extended GeNN to allow the same approach to be used for generating efficient, parallel model initialisation code from code snippets describing state variable and synaptic connectivity initialisation algorithms (13). Offloading initialisation to the GPU sped up model initialisation by around $20\times$ on a desktop PC (13), suggesting that these initialisation algorithms are well-suited to GPU acceleration. (TODO: something explaining why this is for synapses) In fact, it seems somewhat illogical to run these algorithms only once to fill the limited memory of the GPU with data only to then read it back throughout the simulation and in so doing, overload the limited memory bandwidth.

What if we could instead ‘procedurally’ generate connectivity and synaptic weights ‘on the go’ as spikes are triggered? If we could do this in less than than the 80 instructions required to hide the memory latency in the current approach, this new approach could be *faster* as well as requiring no memory to store connectivity and synaptic weights. Although this idea has not been previously applied to modern hardware, Eugene Izhivich used a similar approach for simulating an extremely large thalamo-cortical model with 1×10^{11} neurons and 1×10^{15} synapses on a modest PC cluster in 2005 (TODO: cite). Sadly, while this remains an incredible achievement, simulating the model for 1 second of biological time required 50 days of simulation. However, high-end GPUs have thousands of times more compute power than the CPUs available in 2005 and, due to the limited memory bandwidth available to each of their parallel computing elements, are particularly well-suited to this approach.

To demonstrate the performance and scalability of our ‘procedurally’ generate connectivity, we used a network, initially designed as a medium for experimentation into signal propagation through cortical networks (16), but subsequently widely used as a scalable benchmark (17). The network consists of N integrate-and-fire neurons, partitioned into $\frac{4N}{5}$ excitatory and $\frac{N}{5}$ inhibitory neurons. The populations are connected all-to-all with a fixed $P_{\text{conn}} = 10\%$ probability of a synapse existing between a pair of neurons, meaning that the postsynaptic targets of a presynaptic neuron can be modelled using a Bernoulli distribution $\text{Bern}[P_{\text{conn}}]$. The Bernoulli distribution can be sampled by repeatedly drawing from the uniform distribution

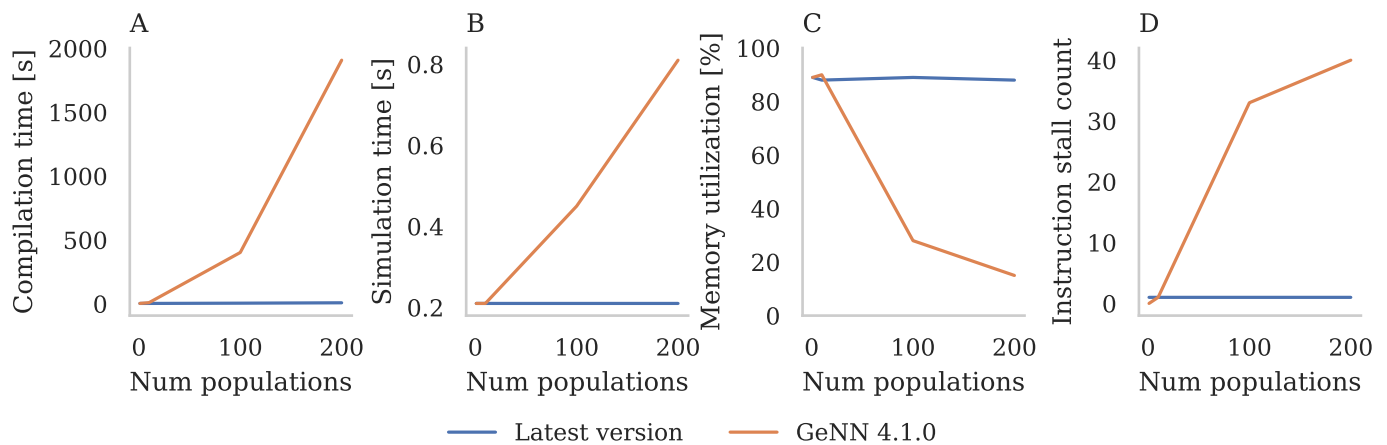


Fig. 2. Performance of a simulation of 1 000 000 LIF neurons driven by a gaussian input current, partitioned into varying numbers of populations. **A** Compilation time using GCC 7.5.0. **B** Simulation time for an 1 s simulation. **C** Memory throughput reported by NVIDIA Nsight compute profiler 'Speed of light' metric. **D** Number of 'No instruction' stalls reported by NVIDIA Nsight compute profiler.

Unif[0,1] and comparing each sample to P_{conn} , but this is inefficient for sparse connectivity. Instead we can sample from the geometric distribution $\text{Geom}[P_{\text{conn}}]$ which describes how the number of Bernoulli trials required to get a success (i.e. a synapse) is distributed. The geometric distribution can be sampled in constant time by inverting the cumulative density function (CDF) of the equivalent continuous distribution (the exponential distribution) to obtain $\frac{\log(\text{Unif}[0,1])}{\log(1-P_{\text{conn}})}$ (18, p499). Therefore, as long as one has the ability to generate a unique but repeatable stream of random numbers for each presynaptic neuron, the postsynaptic targets of a presynaptic neuron can be 'procedurally' generated in parallel. While suitable random number streams *could* be provided by a 'conventional' random number generator (RNG), each presynaptic neurons would need to maintain its own RNG state which would have a significant memory overhead. Instead, we use a 'counter-based' Philox4x32-10 RNG (19). Counter-based RNGs are designed for parallel applications and essentially consist of a pseudo-random bijective function which takes a counter as an input (in this case a 128 bit number) and outputs random numbers. In contrast to conventional RNGs, this means that generating the n^{th} random number in a stream has exactly the same cost as generating the 'next' random number, allowing us to trivially divide up the random number stream between multiple parallel processes (in this case presynaptic neurons). **(TODO: do we need some more explanation of how you get from this to a network simulation?)**

We ran simulations of this network at scales ranging from 1×10^3 to 1×10^6 neurons (corresponding to 100×10^3 and 100×10^9 synapses respectively) on a selection of modern NVIDIA GPU hardware:

Jetson TX2 a low-power embedded system designed for robotic applications with 8 GB of shared memory

Geforce MX130 a laptop GPU with 2 GB of dedicated memory

Geforce GTX 1650 a low-end desktop GPU with 4 GB of dedicated memory

Titan RTX a high-end workstation GPU with 24 GB of dedicated memory

In Fig. 1 we compare the duration of these simulations using our new procedural approach against the standard approach

of storing synaptic connections in memory using two different data structures. Both data structures are described in more detail in our previous work (13) but briefly, in the 'sparse' data structure, a presynaptic neuron's postsynaptic targets are represented as a sorted array of indices whereas, in the 'bitfield' data structure, they are represented as '1s' in a bitfield with a bit for each postsynaptic neuron. None of the devices have enough memory to store the 100×10^9 synapses required for the largest scale using either data structure but, at the 100×10^3 neuron scale, the bitfield data structure allows the model to fit into the memory of several devices it otherwise would not. However, not only is the new procedural approach the *only* way of simulating models at the largest scales but, as Fig. 1 illustrates, even at smaller scales its performance is competitive with and sometime better than the standard approach.

Kernel merging. While the procedural connectivity approach presented in the previous section allows us to simulate models which would otherwise not fit within the memory of a single GPU, there are additional problems when using code generation to generate simulation code for models with large numbers of neuron and synapse populations.

GeNN and – to the best of our knowledge (20) – all other SNN simulators which use code generation to generate all of their simulation code (as opposed to, for example NESTML (21), which uses code generation to generate neuron simulation code) generate separate pieces of code to simulate each population of neurons and synapses. This approach allows optimizations such as the hard-coding of constant parameters to be easily performed and, although generating code for models with many populations will result in large code size, C++ CPU code can be easily divided between multiple modules and compiled in parallel, minimizing the effect on build time. However, GPUs can only run a small number of kernels – which are equivalent to modules in this context – simultaneously (128 on the latest NVIDIA GPUs (**TODO: cite**)). Therefore, in GeNN, multiple neuron populations are simulated within each kernel, resulting in code of the form shown in the following pseudocode which illustrates how 3 populations of 1000 neurons could be simulated in a single

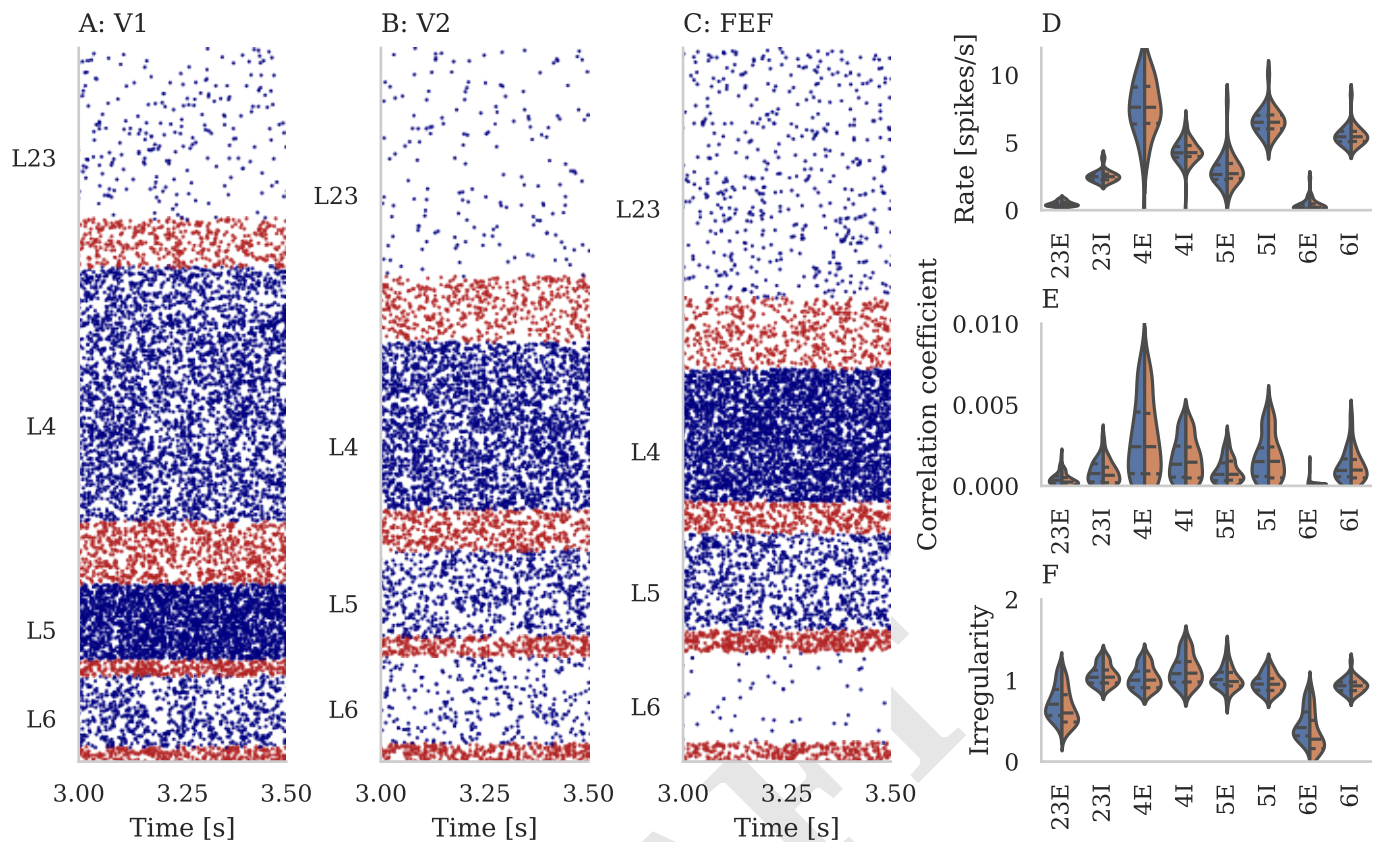


Fig. 3. Results of full-scale multi-area model simulation. **A-C** Raster plots of spiking activity of 3% of the neurons in area V1 **A**, V2 **B**, and FEF **C**. Blue: excitatory neurons, red: inhibitory neurons. **D-F** Spiking statistics for each population across all 32 areas simulated using GeNN and NEST shown as split violin plots. Solid lines: medians, Dashed lines: Interquartile range (IQR). **D** Population-averaged firing rates. **E** Average pairwise correlation coefficients of spiking activity. **F** Irregularity measured by revised local variation LVR (22) averaged across neurons.

kernel: (TODO: very minimal sentence about SIMT here)

```
void updateNeurons()
{
    if(thread < 1000) {
        // Update neuron population A
    }
    else if(thread >= 1000 && thread < 2000) {
        // Update neuron population B
    }
    else if(thread >= 2000 && thread < 3000) {
        // Update neuron population C
    }
}
```

This approach works well for models with small numbers of populations but, as Fig. 2A illustrates, when we partition a model consisting of 1 000 000 LIF neurons into a large number of populations (increasing the size of the neuron kernel), compilation times increases super-linearly – quickly becoming impractical. Furthermore, Fig. 2B shows that when the model is partitioned into a large number of populations, the simulation also runs much more slowly. We would expect this model to be memory bound as each thread in the model reads 32 B of data and, as we discussed previously, hiding the latency of these memory accesses would require approximately 320 arithmetic operations which is many more than are required

to sample from the uniform distribution and update a LIF neuron. Fig. 2C – obtained using data from the NVIDIA Nsight compute profiler (TODO: cite) – shows that this to be true with the memory system being around 90 % utilised for small numbers of populations. However, when the model is partitioned into large numbers of populations, the kernel stops being able to efficiently use the memory and become latency bound (neither memory or compute are used efficiently). Investigating further using the profiler showed that this drop in performance was accompanied by an increasing number of “No instruction” stalls as shown in Fig. 2D. Stalls are events which prevent the GPU from doing any work during a clock cycle and the profiler documentation suggests that these particular events are likely to be caused by “Excessively jumping across large blocks of assembly code”(TODO: cite) – which makes sense when we are generating kernels with hundreds of thousands of lines of code. (TODO: is more detail required here as to why?)

To address these issues, we developed a new code generator for GeNN which first ‘merges’ the model description, grouping populations which can be simulated using the same generated code. From this merged description, structures are generated to store the pointers to state variables and the parameters which differ between merged populations:

```
struct NeuronUpdateGroup
{
    unsigned int numNeurons;
```

```

275     float* V;
276 };

277 An array of these structures is then declared for each merged
278 population and each element is initialised with pointers to
279 state variables and parameter values:

280 NeuronUpdateGroup neuronUpdateGroup[3];
281 neuronUpdateGroup[0] = {1000, VA};
282 neuronUpdateGroup[1] = {1000, VB};
283 neuronUpdateGroup[2] = {1000, VC};

284 In order for a thread to determine which neuron in which
285 population it should be simulating, we generate an additional
286 data structure – an array containing a cumulative sum of
287 threads used for each population. Each thread performs a
288 simple binary search within this to find the index of the neuron
289 and population it should simulate:

290 unsigned int startThread[3] = {0, 1000, 2000};
291 void updateNeurons()
292 {
293     if(thread < 3000) {
294         // Binary search startThread to determing
295         // which population thread should be
296         // processed. Then update using variables
297         // in neuronUpdateGroup
298     }
299 }

```

As Fig. 2 shows, this approach entirely solves the issues with compilation time and simulation performance caused by large numbers of populations. Therefore, we apply this approach to initialisation and simulation kernels for both neuron and synapse populations.

The multi-area model. Due to lack of computing power and sufficiently detailed connectivity data, previous models of the cortex have either focussed on modelling individual local microcircuits at the level of individual cells (23, 24) or modelling multiple connected areas at a higher level of abstraction where entire ensembles of neurons are described by a small number of differential equations (TODO: find citation). However, data from several species (TODO: find citation) has shown that cortical activity has distinct features at both the global and local levels which can only be captured by modelling interconnected microcircuits at the level of individual cells. The multi-area model (15, 25) does just this – using scaled versions of a previous 4 layer microcircuit model (24) to implement 1 mm² ‘patches’ for each of 32 areas of the macaque cortex involved in visual processing. The 32 areas are connected together with connectivity based on inter-area axon tracing data from the CoCoMac (26) database, further refined using additional anatomical data (27) and heuristics (28) to obtain estimates for the number of synapses connecting pairs of areas. Synapses between areas are then distributed between the populations which make up each area.

By using a supercomputer to simulate a model based on the latest connectivity data and The multi-scale model of the macaque visual cortex (15) developed by

Discussion

- Further scaling - memory only required for neuron parameters

- Learning
- Hardware for procedural connectivity?

Materials and Methods

Please describe your materials and methods here. This can be more than one paragraph, and may contain subsections and equations as required. Authors should include a statement in the methods section describing how readers will be able to access the data in the paper.

- LIF neuron
- Exponential static synapses
- Connectivity
- Parameter values for scaling and merging experiments

Neuron models. The membrane voltage (V_j) of each neuron is modelled as a leaky integrate-and-fire (LIF) unit:

$$\tau_m \frac{dV_j}{dt} = (V_j - V_{rest}) + R_m I_{in_j} \quad [1]$$

where τ_m and R_m represent the time constant and resistance of the neuron’s cell membrane, V_{rest} defines the membrane voltage the neuron returns to if it receives no synaptic input and I_{in_j} represents the input current to the neuron. When the membrane voltage crosses a threshold (V_{thresh}) a spike is emitted, the membrane voltage is reset back to V_{rest} and a countdown timer is started which, while running, disables the integration of further input thus providing a simulated refractory period. Incoming spikes induce an exponentially-shaped input current in I_{in_j} :

$$\tau_{syn} \frac{dI_{in_j}}{dt} = -I_{in_j} + I_{p_j} + \sum_{i=0}^n w_{ij} \sum_{t_i^f} \delta(t - t_i^f) \quad [2]$$

where τ_{syn} represents the time constant with which any spikes (modelled as Dirac delta functions δ) from n presynaptic input neurons occurring at time t are integrated. In addition to its synaptic input, each neuron in the network also receives an independent Poisson input current I_{p_j} (also exponentially shaped by equation 2) which represents input from adjacent cortical regions.

ACKNOWLEDGMENTS. Please include your acknowledgments here, set in a single paragraph. Please do not include any acknowledgments in the Supporting Information, or anywhere else in the manuscript.

1. Herculano-Houzel S, Mota B, Lent R (2006) Cellular scaling rules for rodent brains. *Proceedings of the National Academy of Sciences* 103(32):12138–12143.
2. Gewaltig MO, Diesmann M (2007) NEST (NEural Simulation Tool). *Scholarpedia* 2(4):1430.
3. Carnevale NT, Hines ML (2006) *The NEURON book*. (Cambridge University Press).
4. Jordan J, et al. (2018) Extremely Scalable Spiking Neuronal Network Simulation Code: From Laptops to Exascale Computers. *Frontiers in Neuroinformatics* 12(February):2.
5. Frenkel C, Lefebvre M, Legat JD, Bol D (2018) A 0.086-mm² 12.7-pJ/SOP 64k-Synapse 256-Neuron Online-Learning Digital Spiking Neuromorphic Processor in 28nm CMOS. *IEEE Transactions on Biomedical Circuits and Systems* PP(XX):1–1.
6. Frenkel C, Legat JD, Bol D (2019) A 65-nm 738k-Synapse/mm² Quad-Core Binary-Weight Digital Neuromorphic Processor with Stochastic Spike-Driven Online Learning in 2019 *IEEE International Symposium on Circuits and Systems (ISCAS)*. (IEEE), pp. 1–5.
7. Furber SB, Galluppi F, Temple S, Plana LA (2014) The SpiNNaker Project. *Proceedings of the IEEE* 102(5):652–665.
8. Merolla PA, et al. (2014) A million spiking-neuron integrated circuit with a scalable communication network and interface. *IScience* 345(6197):668–673.
9. Qiao N, et al. (2015) A reconfigurable on-line learning spiking neuromorphic processor comprising 256 neurons and 128k synapses. *Frontiers in Neuroscience* 9(APR):1–17.
10. Schemmel J, Kriener L, Muller P, Meier K (2017) An accelerated analog neuromorphic hardware system emulating NMDA- and calcium-based non-linear dendrites. *Proceedings of the International Joint Conference on Neural Networks* 2017-May:2217–2226.
11. van Albada SJ, Helias M, Diesmann M (2015) Scalability of Asynchronous Networks Is Limited by One-to-One Mapping between Effective Connectivity and Correlations. *PLoS Computational Biology* 11(9):1–37.
12. Rhodes O, et al. (2019) Real-Time Cortical Simulation on Neuromorphic Hardware.
13. Knight JC, Nowotny T (2018) GPUs Outperform Current HPC and Neuromorphic Solutions in Terms of Speed and Energy When Simulating a Highly-Connected Cortical Model. *Frontiers in Neuroscience* 12(December):1–19.
14. Yavuz E, Turner J, Nowotny T (2016) GeNN: a code generation framework for accelerated brain simulations. *Scientific reports* 6(November 2015):18854.

- 384 15. Schmidt M, et al. (2018) A multi-scale layer-resolved spiking network model of resting-state
385 dynamics in macaque visual cortical areas. *PLoS Computational Biology* 14(10):1–38.
- 386 16. Vogels TP, Abbott LF (2005) Signal Propagation and Logic Gating in Networks of Integrate-
387 and-Fire Neurons. *The Journal of Neuroscience* 25(46):10786–10795.
- 388 17. Brette R, et al. (2007) Simulation of networks of spiking neurons: a review of tools and strate-
389 gies. *Journal of computational neuroscience* 23(3):349–98.
- 390 18. Devroye L (2013) *Non-uniform random variate generation*. (Springer-Verlag New York, New
391 York).
- 392 19. Salmon JK, Moraes MA, Dror RO, Shaw DE (2011) Parallel random numbers: As Easy as
393 1, 2, 3 in *Proceedings of 2011 International Conference for High Performance Computing,*
394 *Networking, Storage and Analysis on - SC '11*. (ACM Press, New York, New York, USA),
395 Vol. 81, p. 1.
- 396 20. Blundell I, et al. (2018) Code Generation in Computational Neuroscience: A Review of Tools
397 and Techniques. *Frontiers in Neuroinformatics* 12(November).
- 398 21. Plotnikov D, et al. (2016) NESTML: a modeling language for spiking neurons. pp. 93–108.
- 399 22. Shinomoto S, et al. (2009) Relating neuronal firing patterns to functional differentiation of
400 cerebral cortex. *PLoS Computational Biology* 5(7).
- 401 23. Izhikevich EM, Edelman GM (2008) Large-scale model of mammalian thalamocortical sys-
402 tems. *Proceedings of the National Academy of Sciences of the United States of America*
403 105(9):3593–8.
- 404 24. Potjans TC, Diesmann M (2014) The Cell-Type Specific Cortical Microcircuit: Relating Struc-
405 ture and Activity in a Full-Scale Spiking Network Model. *Cerebral Cortex* 24(3):785–806.
- 406 25. Schmidt M, Bakker R, Hilgetag CC, Diesmann M, van Albada SJ (2018) Multi-scale account
407 of the network structure of macaque visual cortex. *Brain Structure and Function* 223(3):1409–
408 1435.
- 409 26. Bakker R, Wachtler T, Diesmann M (2012) CoCoMac 2.0 and the future of tract-tracing
410 databases. *Frontiers in Neuroinformatics* 6(DEC):1–6.
- 411 27. (2014) A weighted and directed interareal connectivity matrix for macaque cerebral cortex.
412 *Cerebral Cortex* 24(1):17–36.
- 413 28. Ercsey-Ravasz M, et al. (2013) A Predictive Network Model of Cerebral Cortical Connectivity
414 Based on a Distance Rule. *Neuron* 80(1):184–197.